Determination of Parameters of Electron Transport in Dye-Sensitized Solar Cells Using Electrochemical Impedance Spectroscopy

Motonari Adachi,*,† Masaru Sakamoto,‡ Jinting Jiu,§ Yukio Ogata,‡ and Seiji Isoda§

International Innovation Center, Kyoto University, Uji, Kyoto 611-0011, Japan, Institute of Advanced Energy, Kyoto University, Uji, Kyoto 611-0011, Japan, and Institute for Chemical Research, Kyoto University, Uji, Kyoto 611-0011, Japan

Received: March 18, 2006; In Final Form: May 18, 2006

The same equation was derived from two different impedance models based on the quite different physical descriptions proposed by Kern et al.[1] and by Bisquert.[2,3] Reliable values of the parameters relating to electron transport in dye-sensitized solar cells can be determined from measured spectra by electrochemical impedance spectroscopy when careful analysis of the measured spectra is done based on the classification and clarification of the same impedance equation consequent from the two models. The requisites for making highly efficient dye-sensitized solar cells were proposed.

1. Introduction

The kinetics and energetics of transport and recombination in dye-sensitized solar cells (DSSCs) have been investigated over the past several years by using electrochemical impedance spectroscopy (EIS)[1−12] as well as intensity modulated photocurrent spectroscopy (IMPS) and intensity modulated photovoltage spectroscopy (IMVS).[5,11,13−18] "Recombination" in DSSCs is defined in this paper as including and mainly representing the back electron transfer by the back reaction of electrons with oxidized redox species I_3^-. Although much progress has been made in advancing the scientific knowledge of transport and recombination phenomena in porous nanostructured electrodes, the elucidation of processes occurring on dye-sensitized mesoscopic titania electrodes is difficult and remains a topic of current debate.

In this study, we found that the same equation was derived from two different impedance models based on the quite distinct physical descriptions proposed by Kern et al.[1] and by Bisquert.[2,3] Kern et al. reported an analysis of EIS, describing electron transport and charge recombination in nanocrystalline titania films in terms of continuity equations for the conduction band and the trap states, which allows an interpretation of spectra of DSSCs operated in the open circuit under illumination. Their model was based on the experiments with variations in experimental parameters such as the TiO_2 layer thickness, cell thickness, and the charge-transfer resistance of the platinum counter electrode. On the other hand, Bisquert elaborated a general formulation of impedance models mainly from a theoretical viewpoint for electron diffusion and recombination in a thin layer with different boundary conditions, including reflecting boundary conditions at the outer edge of the porous film for the case of DSSCs, covering most of the cases of interest for electronic and electrooptic materials and electrodes. Although these two models give apparently different formulas, the unified equation is derived in this study. The unified equation describes the most important behavior of DSSC, that is, electron transport and charge recombination in nanocrystalline titania electrodes. As mentioned above, the unified equation can express characteristics of the measured spectra obtained from EIS of DSSCs, as shown by Kern et al. and also shown in this work later. Thus, utilizing the mathematical analysis by Bisquert in addition to the above findings, it is possible to apply the unified equation for analysis of measured EIS and determine reliable values of the parameters related to electron transfer and recombination. Since the parameters are determined simultaneously under the working state of solar cells in the case of EIS measurements, establishment of the analytical procedure for determination of reliable values of the parameters enables understanding of the complex electron-transfer phenomena and contributes greatly to elucidate the processes occurring on the titania electrodes of dye-sensitized solar cells.

To apply the equation for practical analysis of EIS, classification and clarification of characteristics of the impedance equation were done. This is very important for analysis to get reliable values of the parameters from the measured spectra of EIS; for example, the peak frequency of the semicircle, ω_{max}, in a Nyquist plot gives a simple relationship with the reaction rate constant for the recombination with tri-iodide, k_{eff}, and the direct current resistance at $\omega = 0$ is given by a simple function of both the electron transport resistance, R_w, and the charge-transfer resistance related to recombination of electrons at the TiO_2/electrolyte interface, R_k.

We present that reliable values of the parameters related to electron transport and recombination, such as k_{eff}, R_k, R_w, and the effective diffusion coefficient of electrons, D_{eff}, can be determined simultaneously from the working state of solar cells when careful analysis of the spectra of EIS measured under the open circuit voltage under the various experimental conditions was done based on the information obtained by classification and clarification of characteristics of the impedance equation. Also, we proposed the conditions for making highly efficient dye-sensitized solar cells using the above analysis and simulations.

* Corresponding author. Present address: International Innovation Center, Kyoto University, c/o Isoda Laboratory, The Institute for Chemical Research, Kyoto University, Uji, Kyoto 611-0011, Japan. Phone: 81-774-38-4538. Fax: 81-774-38-3055. E-mail: adachi@iae.kyoto-u.ac.jp.

† International Innovation Center.

‡ Institute of Advanced Energy.

§ Institute for Chemical Research.

10.1021/jp061693u CCC: $33.50
Published on Web 06/22/2006

2. Experimental Section

2.1. Formation of TiO_2 Nanoscale Materials. We used three kinds of TiO_2 nanoscale materials, that is, (1) nanocrystalline TiO_2 (NC-TiO_2) prepared with a mixed template of the tri-block copolymer F127 [poly(ethylene oxide)$_{106}$−poly(propylene oxide)$_{70}$−poly(ethylene oxide)$_{106}$] and the surfactant CTAB (cetyltrimethylammonium bromide), (2) a TiO_2 network structure of single-crystal-like nanowires (TiO_2-NW), and (3) P-25 (Nippon Aerosil). NC-TiO_2 and TiO_2-NW were prepared after our previous reports, namely, refs 19 and 20, respectively.

2.2. Fabrication of Dye-Sensitized Solar Cells. Thin titania films were prepared by applying a titania gel on a indium−tin−oxide (ITO) conductive glass plate donated by Geomatec Co. Ltd. Thick TiO_2 films were fabricated by repetitive coating and calcination at 723 K for 10 min. The film was calcined last at 723 K for 50 min. The film was then immersed in an ethanol solution of the ruthenium dye *cis*-di(thiocyanato)-*N*,*N*′-bis(2,2′-bipyridyl-4-carboxylate-4′-tetra-butylammonium carboxylate)-ruthenium(II) (N719, Solaronix) overnight for adsorption of the dye. The concentration of the dye was 3×10^{-4} M. As a counter electrode, a platinum electrode was used. A thin Pt layer was deposited on a conductive glass substrate by the sputtering technique using an auto-fine coater (JFC-1600, JEOL).

A sandwich-type cell was assembled to measure the photoelectrochemical properties and impedance of the dye-sensitized solar cells. As an electrolyte solution, 0.05 M of I_2, 0.5 M LiI, and 0.5 M 4-*tert*-butylpyridine (TBP) in 3-methyl-2-oxazolidinone (NMO)/acetonitrile was used mostly. The volume ratio of NMO to acetonitrile was 1/9. A 50 μm thick thermoplastic resin film (Du Pont-Mitsui Polychemicals Co. Ltd.) with a 7 mm × 7 mm window was sandwiched between the titania electrode and the platinum electrode. The assembly was heated on a hot plate to tighten the seal. The electrolyte solution was filled between the two electrodes.

2.3. Photoelectrochemical Measurement. The photocurrent−voltage characteristics were measured using a potentiostat (Hokuto Denko HA-501G, HB-105) by irradiating with simulated solar light, that is, AM 1.5 100 mW/cm^2 (ORIEL 1000W 91192). The cell size was 5 mm × 5 mm. The impedance of the cells was measured by using a frequency response analyzer (Solartron 1255A). The impedance measurements in this study were carried out applying bias of the open circuit voltage, V_{oc}, namely, under the conditions of no electric current. Impedance measurement of cells was recorded in a frequency range from 0.05 Hz to 1 MHz with an ac amplitude of 10 mV.

3. Identity of the Bisquert Equation with the Equation Obtained by Kern et al.

Bisquert[2] obtained the impedance of diffusion and recombination based on the following three assumptions: (1) electrons in the conduction band diffuse, (2) there is no trap, and (3) an irreversible first-order reaction is assumed for the recombination.

The diffusion−recombination model for small amplitude oscillating quantities, superimposed to a given stationary state, is written as

$$\frac{\partial \tilde{n}}{\partial t} = -\frac{\partial \tilde{J}}{\partial x} - k\tilde{n} = D\frac{\partial^2 \tilde{n}}{\partial x^2} - k\tilde{n} \tag{1}$$

$\tilde{n}$, D, and k represent the small oscillating electron density, diffusion coefficient of an electron in the TiO_2 nanocrystal, and reaction rate constant for recombination, respectively.

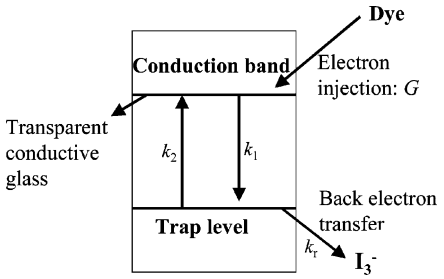

Figure 1. Reaction paths in the TiO_2 electrode of the DSSCs in the model of Kern et al.[1]

The boundary condition is given as

$$\text{At } x = L, \frac{\partial \tilde{n}}{\partial x} = 0 \tag{2}$$

where L represents the film thickness of TiO_2.

The impedance under boundary condition 2 is given by Bisquert as

$$Z = \left(\frac{R_w R_k}{1 + \frac{i\omega}{\omega_k}}\right)^{1/2} \coth\left[\left(\frac{\omega_k}{\omega_d}\right)^{1/2}\left(1 + \frac{i\omega}{\omega_k}\right)^{1/2}\right] \tag{3}$$

where

$$\omega_d = D/L^2, \omega_k = k = 1/\tau \tag{4}$$

$$R_w = \text{Con}\frac{L}{D}, \text{Con} = \frac{k_B T}{q^2 A n_s}, R_k = \frac{\omega_d}{\omega_k} R_w = \text{Con}\frac{1}{Lk} \tag{5}$$

Here, Z, R_w, R_k, τ, k_B, T, q, A, and n_s represent the impedance, electron transport resistance in TiO_2, charge-transfer resistance related to recombination of an electron, lifetime of an electron in TiO_2, Boltzmann constant, absolute temperature, charge of a proton, the electrode area, and the electron density at the steady state in the conduction band, respectively.

Equation 3 can be rewritten, and eq 6 was obtained.

$$Z = R_w\left(\frac{1}{\left(\frac{\omega_k}{\omega_d}\right)\left(1 + \frac{i\omega}{\omega_k}\right)}\right)^{1/2} \coth\left[\left(\frac{\omega_k}{\omega_d}\right)\left(1 + \frac{i\omega}{\omega_k}\right)\right]^{1/2} \tag{6}$$

On the other hand, Kern et al.[1] derived the impedance of diffusion and recombination in TiO_2 based on the reaction paths shown in Figure 1. They set the following three assumptions: (1) electrons are injected into the conduction band from the excited dye at the injection rate G under illumination, (2) only a single trap level is assumed, and the rate constant, k_1, for the trapping of the conduction band electrons is much faster than k_2 for the detrapping of the electrons, and (3) trapped electrons are lost by the recombination with I_3^-, and the second-order reaction rate is assumed with respect to electrons for the recombination.

The continuity equations for the conduction band electrons and for the electrons in the trap state, which describes injection, diffusion, collection, trapping, detrapping, and recombination of electrons in the TiO_2 of the DSSCs, are given as

$$\frac{\partial n}{\partial t} = D_{cb}\frac{\partial^2 n}{\partial x^2} - k_1 n + k_2 N + G \tag{7}$$

$$\frac{\partial N}{\partial t} = -k_2 N - k_r N^2 + k_1 n \tag{8}$$

$$n = n_s + \Delta n \exp(i\omega t) \tag{9}$$

$$N = N_s + \Delta N \exp(i(\omega t + \varphi)) \tag{10}$$

where D_{cb} represents the diffusion coefficient of an electron in the conduction band and n_s and N_s are the steady state electron density in the conduction band and in the trap state, respectively. Δn and ΔN are the amplitudes of the modulated component of the conduction band and trap state electron density, respectively.

Defining

$$D_{eff} = D_{cb}\frac{k_2}{k_1} \tag{11}$$

$$k_{eff} = 2N_s k_r \tag{12}$$

$$\gamma^2 = \frac{k_{eff}}{D_{eff}} + \frac{i\omega}{D_{eff}} \tag{13}$$

and using the following boundary conditions

$$\text{at } x = 0,\ qD_{eff}\left(\frac{\partial \Delta n}{\partial x}\right) = \frac{\Delta I}{A} = \Delta J \tag{14}$$

$$\text{at } x = L,\ \frac{\partial \Delta n}{\partial x} = 0 \tag{15}$$

impedance is obtained by Kern et al. as

$$Z = -S\frac{1}{qA}\frac{1}{D_{eff}\gamma\sqrt{1/k_{eff}}}\frac{1 + e^{2\gamma L}}{1 - e^{2\gamma L}} \tag{16}$$

where

$$S = \frac{k_B T}{q n_s}\sqrt{1/k_{eff}} \tag{17}$$

Equation 16 was transformed into eq 20 as follows.

Defining

$$\omega_d = \frac{D_{eff}}{L^2},\ \omega_k = k_{eff} \tag{18}$$

$$\gamma L = \sqrt{\frac{\omega_k}{\omega_d} + \frac{i\omega}{\omega_d}} \tag{19}$$

and impedance can be rewritten as

$$Z = R_w\left(\frac{1}{\left(\frac{\omega_k}{\omega_d}\right)\left(1 + \frac{i\omega}{\omega_k}\right)}\right)^{1/2}\coth\left[\left(\frac{\omega_k}{\omega_d}\right)\left(1 + \frac{i\omega}{\omega_k}\right)\right]^{1/2} \tag{20}$$

where

$$R_w = \frac{k_B T}{q^2 A n_s}\frac{L}{D_{eff}} = \mathrm{Con}\frac{L}{D_{eff}},\ R_k = \mathrm{Con}\frac{1}{L k_{eff}} \tag{21}$$

Then, eq 20 becomes the same as eq 6.

Let us consider here the reason why the impedance by Kern et al. becomes the same as the equation by Bisquert. The assumption that the trapping is much faster than detrapping ($k_1 \gg k_2$) results in $N_s \gg n_s$. Electrons in the trap state N detrap to the conduction band and diffuse with the diffusion coefficient D_{cb} for the period proportional to k_2/k_1. Thus, electrons in the trap state are regarded as diffusing charges with the diffusion constant $D_{eff} = D_{cb}(k_2/k_1)$. Electrons in the trap state also react with I_3^- with a pseudo-first-order reaction rate with reaction rate constant $k_{eff} = 2N_s k_r$. Therefore, the model by Kern et al. is simplified as follows: injected electrons become the trap electrons, diffusing with the diffusion coefficient D_{eff} and being lost by the pseudo-first-order recombination rate with the rate constant k_{eff}. This reaction scheme is eventually the same as that of Bisquert.

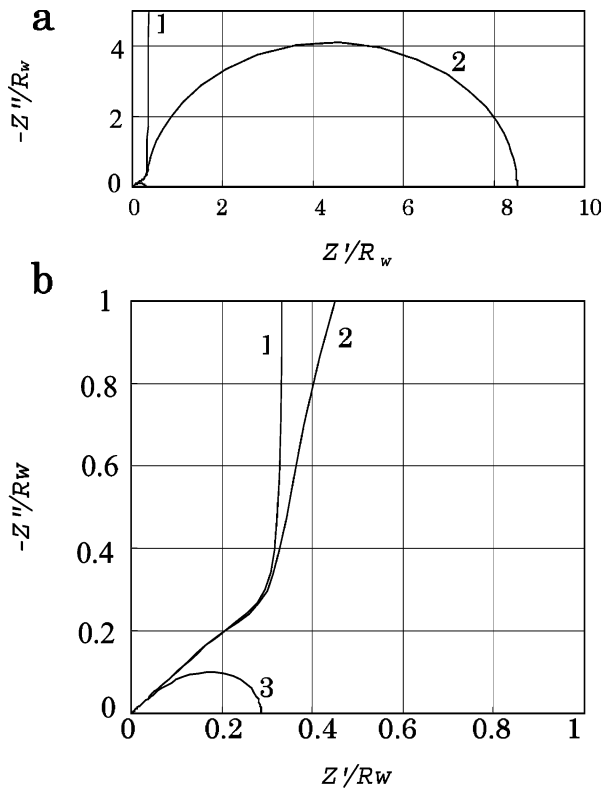

Figure 2. Nyquist plot of the impedance (eq 20) for diffusion coupled with a recombination reaction under the reflecting boundary condition. Part b shows magnification of a part of part a. Curves 1, 2, and 3 show the calculated ones of eqs 22, 25, and 28, respectively.

4. Classification and Clarification of Characteristics of the Impedance Equations of TiO_2 Electrodes

Since the impedance equation (eq 20) can express characteristics of measured spectra obtained from EIS of DSSCs, classification and clarification of characteristics of the impedance equation are very important for analysis of the measured spectra of EIS. Equation 20 indicates that the shape of the impedance in a Nyquist plot is determined by only one parameter, $(\omega_d/\omega_k) = (R_k/R_w)$. We can classify the equation into the following three cases after Bisquert,[2] as shown in Figure 2, which shows Nyquist plots of the impedance equation (eq 20).

(1) $R_k \rightarrow \infty$: the limiting case leads to simple diffusion, namely, eq 22 shown by curve 1 of Figure 2.

$$Z = R_w\sqrt{\frac{\omega_d}{i\omega}}\coth\sqrt{\frac{i\omega}{\omega_d}} \tag{22}$$

When ω becomes large,

$$Z = R_w\sqrt{\frac{\omega_d}{i\omega}} = R_w\left(\sqrt{\frac{\omega_d}{2\omega}} - i\sqrt{\frac{\omega_d}{2\omega}}\right) \tag{23}$$

Thus, the real part, Z', of impedance Z is equal to the minus imaginary part, $-Z''$, of impedance Z.

When ω becomes small,

$$Z = R_w\left(\frac{1}{3} - i\frac{\omega_d}{\omega}\right) \tag{24}$$

Thus, Z' approaches $(^1/_3)R_w$ and Z'' becomes ∞.

(2) $R_k \gg R_w$: when the reaction resistance, R_k, is finite and the frequency is high ($\omega \gg \omega_d$), eq 20 is simplified to eq 23. When the frequency is low ($\omega \ll \omega_d$), eq 20 is expressed by eq 25:

$$Z = \frac{1}{3}R_w + \frac{R_k}{1 + \frac{i\omega}{\omega_k}} \tag{25}$$

Therefore, the impedance is shown in a Nyquist plot by curve 2 in Figure 2. There is a small increase part along the straight line of $Z' = -Z''$ at high frequency and a large arc at low frequency. The latter corresponds to the recombination process, which is much slower than diffusion through the TiO_2 layer in this case ($R_k \gg R_w$, $\omega_d \gg \omega_k$).

Two important relationships for analysis of measured EIS are derived from eq 25. The peak frequency of an arc in a Nyquist plot, ω_{max}, is given as

$$\omega_{max} = k_{eff} \tag{26}$$

The dc resistance, R_{dc}, at $\omega = 0$ is given as

$$R_{dc} = \frac{1}{3}R_w + R_k \tag{27}$$

(3) $R_k \ll R_w$: eq 20 leads to the following function:

$$Z = \sqrt{\frac{R_w R_k}{1 + \frac{i\omega}{\omega_k}}} \tag{28}$$

The impedance is shown by curve 3 in a Nyquist plot of Figure 2. In this case, the recombination time is shorter than the time for diffusion across the TiO_2 layer ($R_k \ll R_w$, $\omega_d \ll \omega_k$). Thus, this case must be avoided for attainment of the highly efficient cells. Since the concentration profile collapses and the electron density becomes very small in the middle of the TiO_2 layer in this case, eq 28 describes the diffusion and recombination in semi-infinite space.

The following two relationships are derived from eq 28.

$$\omega_{max} = \sqrt{3}k_{eff} \tag{29}$$

$$R_{dc} = (R_w R_k)^{1/2} \tag{30}$$

The calculations of eq 20 with various combinations of R_w, R_k, D_{eff}, and k_{eff} show that the shapes in a Nyquist plot of the impedance under different conditions become exactly the same one as long as the value of R_k/R_w is the same. Also, the calculation of eq 20 confirms the validity of eqs 23 and 25−30.

5. Determination of Parameters of Electron Transport

Figure 3 shows a typical experimental spectrum of EIS of our DSSCs. Three arcs in the Nyquist plot were observed with peak frequencies of $\omega_{max} = 6.3$ kHz, 12 Hz, and around 1 Hz.

5.1. Influence of Pt Thickness and Assignment of Arcs. To assign the arc corresponding to the electron transfer at the Pt counter electrode, EIS of the cell made of two Pt electrodes and electrolyte was measured. The thickness of the Pt film on ITO glass was varied by changing the sputtering time. The thicker one was sputtered for 7 min and the thinner one for 25 s with a current of 40 mA. The obtained Nyquist plot under zero bias voltage is shown in Figure 4. Two peaks at 4 kHz and around 0.6−0.8 Hz were observed for both cases. The resistance of the higher frequency arc changed significantly with the variation in the thickness of the Pt film, namely, 6.5 Ω for the thicker one and 53 Ω for the thinner one. Thus, we can conclude that the arc with 4−6 kHz is assigned to the impedance of the electron transfer at the Pt counter electrode. This assignment is consistent with the result reported previously by Kern et al.[1] and by many other reports.[4,8−10,21]

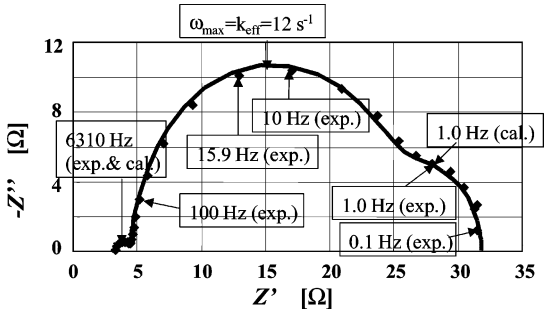

Figure 3. Example of the measured spectrum of EIS of DSSCs made of P-25. Diamond-shaped symbols show the experimental points in the Nyquist plot. The solid curve shows the calculated one.

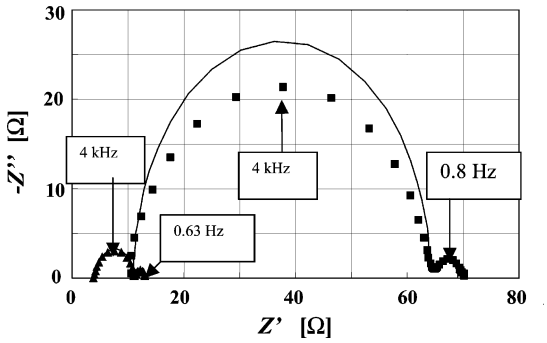

Figure 4. Spectra of EIS for the cell made of two Pt electrodes, which sandwiched the electrolyte. Key: (▲) thicker Pt film; (■) thinner Pt film.

For the small arcs in the low frequency range 0.6−1 Hz, the many previous reports[1,6−10,21] concluded that the arc was the finite Warburg impedance of tri-iodide in electrolyte. The good agreement of the diffusion coefficient of I_3^- determined from the diffusion-limited current and those determined from the finite Warburg impedance strongly supports the assignment of this arc.[8]

5.2. Models of the Impedance of the Electron Transfer at the Pt Counter Electrode and the Finite Warburg Impedance of Tri-Iodide in Electrolyte. As shown in Figure 3, the measured spectra of EIS of DSSCs include the impedance of the electron transfer at the Pt counter electrode and the finite Warburg impedance of tri-iodide in electrolyte.

The impedance of the electron transfer at the Pt counter electrode can be described approximately by the following simple RC circuit.

$$Z_p = \frac{1}{\frac{1}{r_p} + i\omega C_p} \tag{31}$$

$$\omega_{max} = \frac{1}{r_p C_p} \tag{32}$$

where r_p and C_p represent the resistance at the Pt surface and the capacitance at the Pt surface, respectively.

The finite Warburg impedance describes the diffusion of tri-iodide ions in the electrolyte.[1,8]

$$Z_N = R_D \frac{1}{\sqrt{\frac{i\omega}{(D_l/\delta^2)}}} \tanh \sqrt{\frac{i\omega}{(D_l/\delta^2)}} \tag{33}$$

$$R_D = \frac{k_B T}{m^2 q^2 A_V C^* D_l \delta} \tag{34}$$

$$\omega_{max} \approx 2.5 \frac{D_l}{\delta^2} \tag{35}$$

where D_l and δ represent the diffusion coefficient of I_3^- and the thickness of the liquid film, respectively. The number of electrons transferred in each reaction, m, is 2 in this case. A_V and C^* are Avogadro's constant and the concentration of I_3^- in the bulk, respectively.

The solid curves in Figure 4 are the calculated curves using eqs 31 and 33. The calculated curves simulate roughly the spectra obtained by experiments, although some deviation is observed for the impedance at the Pt electrode due to the too simple RC circuit model.

Since the impedance at the Pt electrode, Z_p, and the impedance of the diffusion of tri-iodide in the electrolyte, Z_N, are described by eqs 31 and 33, the total impedance of the DSSC, Z_S, is given as the summation of the impedance of diffusion and recombination in the TiO_2 electrode, Z, given by eq 20, Z_p, and Z_N.

$$Z_S = Z + Z_p + Z_N \tag{36}$$

The characteristics of the impedance equation of the TiO_2 electrode, Z, which is described in section 4, was confirmed to be held even in eq 36.

5.3. Procedure for Determination/Estimation of Parameters of Electron Transport. Parameters of electron transport can be determined/estimated from a Nyquist plot obtained experimentally, such as the one being shown in Figure 3.

(1) Parameters included in the impedance equation of the TiO_2 electrode can be obtained from the central arc as follows.

(1-1) k_{eff} is estimated from the peak frequency, ω_{max}, of the central arc (in the 10−100 Hz range) using eq 26.

(1-2) R_k is estimated from the diameter of the central arc using eqs 25 and 27.

(1-3) The measured value of the TiO_2 film thickness is used as L.

(1-4) Con is estimated from eq 21 as $\mathrm{Con} = R_k L k_{eff}$.

(1-5) R_k/R_w is estimated from the shape of the central arc. When the arc is a true circle, R_k is much larger than R_w. When the arc in the high frequency range is expressed by curve 3 shown in Figure 2b, the relationship between R_k and R_w is expressed as $R_k \approx R_w$ or $R_k < R_w$.

(1-6) D_{eff} is estimated from eq 21 as follows:

$$D_{eff} = \left(\frac{R_k}{R_w}\right) L^2 k_{eff}$$

(2) The parameters included in the impedance at the Pt electrode can be obtained from the high frequency arc as follows.

(2-1) r_p is estimated from the diameter of the high frequency arc (in the kHz range).

(2-2) C_p is estimated from eq 32 using the peak frequency of the high frequency arc as

$$C_p = \frac{1}{r_p \omega_{max}}$$

(3) The parameters included in the impedance of the diffusion of tri-iodide in electrolyte can be obtained from the low frequency arc as follows.

(3-1) R_D in eq 33 is estimated from the diameter of the low frequency arc (in the mHz range).

(3-2) The thickness of the thermoplastic resin film is used as δ.

(3-3) D_l is estimated from eq 35 using the peak frequency of the low frequency arc, ω_{max}, as

$$D_l = (1/2.5)\delta^2 \omega_{max}$$

5.4. Practical Illustration of Determination/Estimation of the Parameters of the Measured Spectrum of EIS of DSSCs. Figure 3 shows an example of the measured spectrum of EIS of DSSCs made of P-25. We present an example of determination/estimation of the parameters of electron transfer from the experimental spectrum shown in Figure 3.

(1) The parameters included in the impedance equation of the TiO_2 electrode were determined/estimated as follows from the central arc in Figure 3.

(1-1) The peak frequency of the central arc, ω_{max}, was determined as 12 Hz. Thus, we estimated k_{eff} as 12 s^{-1}.

(1-2) The diameter of the central arc in Figure 3 was estimated as 19.5 Ω. Thus, we determined R_k as 19.5 Ω.

(1-3) L was given as 3.85 μm from the measurement of the film thickness of TiO_2.

(1-4) Con was calculated as 0.09 Ω cm s^{-1} from the equation $\mathrm{Con} = R_k L k_{eff}$.

(1-5) Since the shape of the central arc is a true circle, R_k/R_w was estimated to be higher than 10.

(1-6) D_{eff} was estimated from the equation

$$D_{eff} = \left(\frac{R_k}{R_w}\right) L^2 k_{eff}$$

When $R_k/R_w = 10$, D_{eff} was calculated as 1.8×10^{-5} cm^2/s. When $R_k/R_w = 30$, D_{eff} became 5.3×10^{-5} cm^2/s. The values of R_k/R_w and D_{eff} were determined by the trial-and-error method. In the case of R_k/R_w being too high, $R_k/R_w \gg 10$, the determination of R_k/R_w and D_{eff} becomes difficult, as shown later in simulation.

(2) The parameters included in the impedance at the Pt electrode were determined/estimated from the high frequency arc in Figure 3 as follows.

(2-1) r_p was estimated as 1 Ω from the diameter of the high frequency arc.

(2-2) Since ω_{max} was given as 6.3 kHz from the high frequency arc, C_p was estimated as 160 μF from the equation

$$C_p = \frac{1}{r_p \omega_{max}}$$

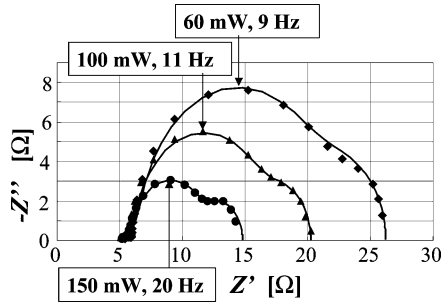

Figure 5. Effect of the light intensity of the irradiation light. P-25 cells were used. Key: (◆) 60 mW; (▲) 100 mW; (●) 150 mW; (—) calculated curves using the parameters shown in Table 1.

(3) The parameters included in the impedance of the diffusion of tri-iodide in electrolyte were determined/estimated from the low frequency arc in Figure 3 as follows.

(3-1) The dc resistance of the impedance of diffusion of I_3^- in electrolyte, R_D, was estimated as 8 Ω from the diameter of the low frequency arc.

(3-2) δ was given as 50 μm from the thickness of the thermoplastic resin.

(3-3) D_l was calculated as 1×10^{-5} cm^2/s from the equation $D_l = (1/2.5)\delta^2\omega_{max}$, assuming the ω_{max} value of the arc was 1 Hz.

The solid curve in Figure 3 is the calculated one using eq 36 with eqs 20, 31, and 33. After several trials, R_k/R_w and D_{eff} were determined as 15 and 2.67×10^{-5} cm^2/s, respectively. All other parameters estimated above were used for the calculation. Thus, we can determine reliable values of the parameters when careful analysis of the measured spectra of EIS is done based on the information described in section 4.

5.5. Determination of the Parameters of Electron Transport under Various Experimental Conditions and Some Insights into Highly Efficient Cells. The parameters of the electron transport in DSSCs were determined by the procedure described above from the EIS measurements under the various experimental conditions, namely, the light intensity of the irradiation light, TiO_2 film thickness, addition of TBP, concentration of iodine, and nanoscale titania materials constituting the TiO_2 electrode.

The effect of the light intensity of the irradiation light is shown in Figure 5, where the electrode was made of P-25, and the film thickness was 11.1 μm. With an increase in light intensity, the photocurrent density increased as 6.81 mA cm^{-2} for 60 mW cm^{-2}, 11.32 mA cm^{-2} for 100 mW cm^{-2}, and 17.43 mA cm^{-2} for 150 mW cm^{-2}. The light-to-electricity conversion yield, η, was, however, almost constant around 6.08% for all light intensities. The dc resistance at $\omega = 0$ decreased with an increase in light intensity, for which there are two possible explanations: (1) an increase in the electron density, n_s, which leads to small R_k and R_w, and (2) an increase in the recombination rate, k_{eff}, which leads to small R_k. As shown in Figure 5, the ω_{max} value of the central arc increases with an increase in light intensity, indicating k_{eff} increases with increasing light intensity. Thus, the recombination rate increases with increasing light intensity. This is confirmed by the fact that the value of Con given by eqs 5 and 21 is almost constant, as shown in Table 1. Since Con is inversely proportional to the steady state electron density, n_s, the steady state electron density is almost constant, although injection of electrons increases with increasing light intensity, indicating that electrons are lost rapidly by recombination with an increase in light intensity. This shows

TABLE 1: Properties Determined by Electrochemical Impedance Spectroscopy Measurements[a]

	TiO_2 material	D_{eff} (cm^2 s^{-1})	k_{eff} (s^{-1})	τ_{eff} (s)	R_k (Ω)	R_w (Ω)	Con (Ω cm s^{-1})	R_D (Ω)	n_s (cm^{-3})	film thickness (μm)	J_{sc} (mA cm^{-2})	V_{oc} (V)	fill factor	η (%)
example	P-25	2.67×10^{-5}	12	0.083	19.5	1.3	0.09	8	7.12×10^{18}	3.85	8.58	0.77	0.709	4.69
light intensity	P-25	5.0×10^{-5}	9	0.111	13.5	4.51	0.135	6.5	4.75×10^{18}	11.1	6.81	0.76	0.71	6.09
60 mW cm^{-2}		5.0×10^{-5}	11	0.091	9.58	3.69	0.117	4.7	5.48×10^{18}	11.1	11.32	0.78	0.69	6.08
100 mW cm^{-2}		5.0×10^{-5}	20	0.050	5.18	2.03	0.115	3.8	5.57×10^{18}	11.1	17.43	0.77	0.68	6.04
150 mW cm^{-2}														
film thickness	NC-TiO_2	0.11×10^{-5}	16	0.063	17	16.4	0.07	5	9.16×10^{18}	2.57	9.81	0.79	0.692	5.36
2.57 μm		0.042×10^{-5}	15.5	0.065	27.8	21.2	0.062	5	10.3×10^{18}	1.44	7.00	0.80	0.641	3.59
1.44 μm		0.026×10^{-5}	16	0.063	67	15.4	0.061	5	10.6×10^{18}	0.57	3.45	0.81	0.705	1.97
0.57 μm														
TBP	P-25	5.0×10^{-5}	12.5	0.08	25.9	1.46	0.154	4.6	4.16×10^{18}	4.75	9.69	0.79	0.707	5.41
with														
without		1.0×10^{-5}	40	0.025	21.1	19	0.4	9.7	1.60×10^{18}	4.75	12.15	0.58	0.619	4.36
iodine concn	P-25	4.5×10^{-5}	10	0.100	17.5	0.876	0.083	6	7.72×10^{18}	4.75	10.47	0.75	0.736	5.78
0.05 M		1.0×10^{-5}	40	0.025	12.8	11.5	0.243	4.7	2.64×10^{18}	4.75	6.79	0.70	0.738	3.51
0.5 M														
TiO_2 material	TiO_2-NW	2.7×10^{-5}	11	0.091	9.09	0.454	0.035	3.8	18.3×10^{18}	3.5	10.68	0.74	0.726	5.74
	NC-TiO_2	2.7×10^{-5}	11	0.091	9.35	0.467	0.036	3.8	17.8×10^{18}	3.5	10.65	0.74	0.713	5.62
	P-25	5.0×10^{-5}	16	0.063	41.8	1.64	0.234	5.0	2.73×10^{18}	3.5	6.20	0.75	0.583	2.71
highly efficient cell	NC-TiO_2 (mainly)	10×10^{-5}	6.3	0.161	6.23	0.70	0.053	5.6	12.1×10^{18}	13.5	14.40	0.76	0.72	7.83

[a] All experiments shown here were done at open circuit voltage.

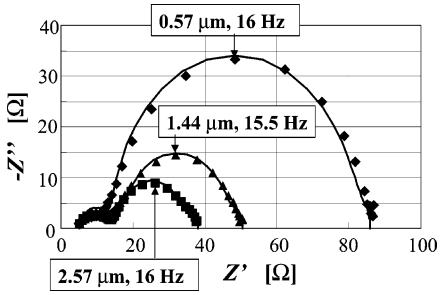

Figure 6. Effect of TiO_2 film thickness. NC-TiO_2 cells were used. Key: (◆) 0.57 μm; (▲) 1.44 μm; (■) 2.57 μm; (—) calculated curves using the parameters shown in Table 1.

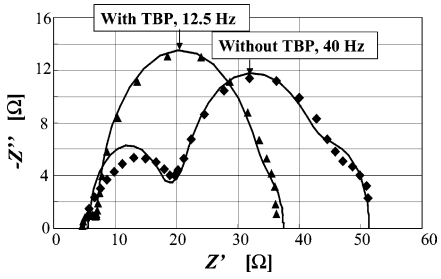

Figure 7. Effect of the addition of TBP. P-25 cells were used. Keys: (▲) with TBP; (◆) without TBP; (—) calculated curves using the parameters shown in Table 1.

the reason the conversion efficiency, η, was almost constant for all light intensities. Fisher et al.[13] have reported similar results.

Figure 6 shows the effect of the TiO_2 film thickness, L, of the cells made of NC-TiO_2. The adsorbed amount of dye increased proportional to L. Even though the film thickness increases, the ω_{max} value of the central arc, namely, the recombination rate, k_{eff}, is constant, as shown in Figure 6. In this case, the n_s value was 2 times higher than that of the cells made of P-25 shown in Figure 5, as shown in Table 1. Since R_k is inversely proportional to L, as shown in eq 21, direct current resistance of the cell decreased with an increase in L. Since the film was rather thin, the current density, J_{sc}, increased proportional to the adsorbed amount of dye, that is, proportional to the film thickness, resulting in an increase in the efficiency, η. Effective diffusion coefficients, D_{eff}, interestingly increase with an increase in film thickness. One possible reason for that is the effect of calcinations, but concrete reasoning needs further work.

The effect of the addition of TBP is shown in Figure 7. As the ω_{max} value of the central arc was 12.5 Hz for the with-TBP case and 40 Hz for the without-TBP case, the recombination rate constant, k_{eff}, in the without-TBP case was about 4 times larger than that in the with-TBP case, indicating clearly the preventing effect of TBP for the recombination reaction by a significant negative potential shift of the band edges due to covering the surface of TiO_2 with TBP.[11,14] As shown in Table 1, the electron density, n_s, in the without-TBP case was less than half of that in the with-TBP case, which means that electrons were lost rapidly in the without-TBP case. A big difference in V_{oc} was also observed in Table 1. The D_{eff} value in the without-TBP case was one-fifth of that in the with-TBP case. This can be understood by the trap model, because a decrease in n_s causes a smaller D_{eff} value. Since the R_w value in the without-TBP case was 13 times larger than that in the with-TBP case, R_k/R_w was 1.11 for the without-TBP case and 17.7 for the with-TBP case. Thus, the shape of the central arc

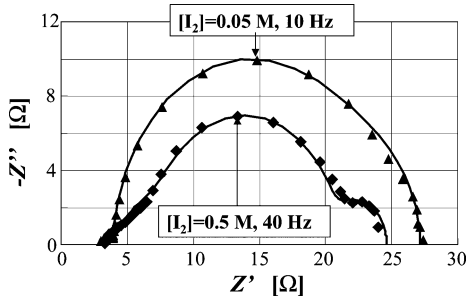

Figure 8. Effect of the concentration of iodine in the electrolyte. P-25 cells were used. Key: (▲) 0.05 M; (◆) 0.5 M; (—) calculated curves using the parameters shown in Table 1.

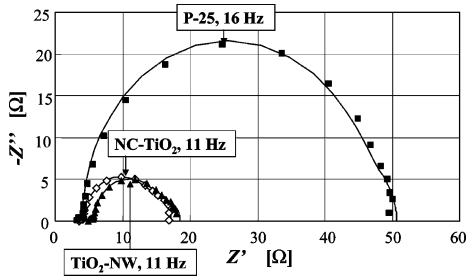

Figure 9. Effect of the TiO_2 materials constituting the TiO_2 electrode. Key: (■) P-25; (◇) NC-TiO_2; (▲) TiO_2-NW; (—) calculated curves using the parameters shown in Table 1.

for the without-TBP case deviated from a true circle especially in the high frequency range.

The effect of iodine concentration is shown in Figure 8. In this case, the ω_{max} value of the central arc was 10 Hz for $[I_2] = 0.05$ M and 40 Hz for $[I_2] = 0.5$ M, as expected. Since the equilibrium constant for the reaction $I_3^- = I_2 + I^-$ was reported[22,23] as $K = [I_3^-]/[I_2][I^-] = 10^{6.78}$, the concentration of I_3^- for $[I_2] = 0.5$ M became 10 times higher than that for $[I_2] = 0.05$ M, indicating that the concentration of tri-iodide ions at the TiO_2/electrolyte interface increased at high iodine concentrations. Thus, k_{eff} in the case of $[I_2] = 0.5$ M was 4 times larger than that in the case of $[I_2] = 0.05$ M. As shown in Table 1, the steady state electron density, n_s, for the case of $[I_2] = 0.5$ M was smaller than one-third of that for the case of $[I_2] = 0.05$ M, resulting in D_{eff} in the case of $[I_2] = 0.5$ M being 1/4.5 of that in the case of $[I_2] = 0.05$ M. R_k/R_w was 1.11 for the case of $[I_2] = 0.5$ M and 19.9 for the case of $[I_2] = 0.05$ M. The shape of the central arc for the case of $[I_2] = 0.5$ M was obviously different from a true circle in comparison with the case of $[I_2] = 0.05$ M.

Figure 9 shows the effect of TiO_2 materials constituting the titania electrode for the same film thickness of 3.5 μm. Here, the characteristics of our two titania materials NC-TiO_2 and TiO_2-NW were compared with P-25. The most remarkable characteristic point between P-25 and our titania was the difference in Con values. The electron density, n_s, of our titania cells was 7 times higher than that of P-25. The recombination rate constants, k_{eff}, of our titania cells were smaller than that of P-25 by 1/1.5, because the ω_{max} values of the central arc were 11 Hz for our cells and 16 Hz for the P-25 cell, as shown in Figure 9. These findings suggest that the adsorbed amount of dye is important. The Brunauer−Emmett−Teller (BET) surface area of NC-TiO_2 and TiO_2-NW was 150−180 m^2/g, which was much higher than the 50 m^2/g value of P-25. The measured amount of dye was 10.8×10^{-8} mol cm^{-2} for NC-TiO_2, 11.8×10^{-8} mol cm^{-2} for TiO_2-NW, and 4.69×10^{-8} mol cm^{-2} for P-25, resulting in a high efficiency of our cells, as shown in Table 1.

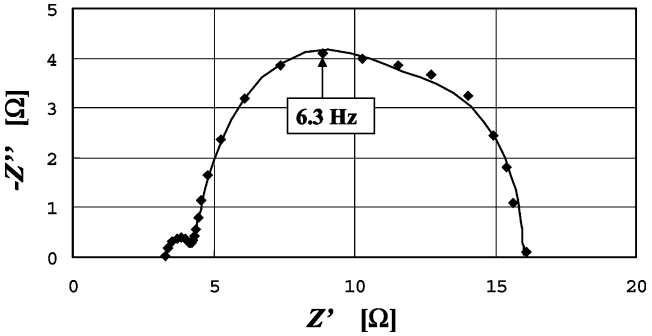

Figure 10. Nyquist plot of the highly efficient complex cell. The cell was made of mainly NC-TiO_2. Key: (—) calculated curves using the parameters shown in Table 1.

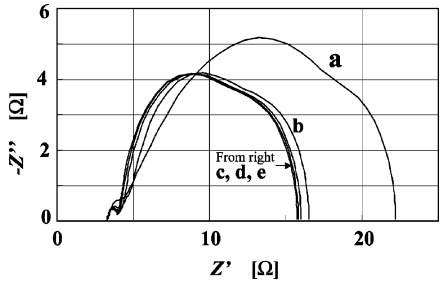

Figure 11. Simulation with variation in D_{eff}. Original $D_{eff} = 9 \times 10^{-5}$ cm^2 s^{-1}. Ratio of D_{eff} to the original D_{eff}: (a) 1/30; (b) 1/3; (c) 1; (d) 3; (e) 30.

Next, we intended to get the characteristics of highly efficient cells and made a highly efficient complex cell made of mainly NC-TiO_2, namely, lower layers made of pure NC-TiO_2 and upper layers made of NC-TiO_2 including 8 wt % P-25. We attained a light-to-electricity conversion yield of $\eta = 7.8\%$. The Nyquist plot of the highly efficient cell is shown in Figure 10. The diameter and ω_{max} values of the central arc were determined as 6.2 Ω and 6.3 Hz, respectively. The calculated curve in Figure 10 was obtained using the values of parameters shown in Table 1. k_{eff} was determined as 6.3 s^{-1}, meaning $\tau_{eff} = 0.16$ s. As shown in Table 1, k_{eff} is the smallest and τ_{eff} is the largest comparing with all the determined k_{eff} and τ_{eff} values in this study. The electron diffusion coefficient, D_{eff}, was obtained as 1.0×10^{-4} cm^2 s^{-1}, which is the highest, as shown in Table 1. This contributes to the low R_w value of 0.70 Ω, resulting in $R_k/R_w = 9.0$, which is high enough. Con was 0.053, meaning that n_s is high.

From the results mentioned above, high D_{eff}, low k_{eff}, high $R_k/R_w = \omega_d/\omega_k$, and low Con corresponding to high n_s are the necessary conditions to attain highly efficient cells.

To get further information for making highly efficient cells, calculations by changing the values of D_{eff} were carried out keeping the same values for other parameters obtained for Figure 10, and the result is shown in Figure 11. The original calculation is shown by curve c. An increase in D_{eff} does not affect the Nyquist plot, but a decrease in D_{eff} changes the shape of the Nyquist plot significantly. This can be explained as follows: R_k/R_w in Figure 10 is 9.0, as mentioned above, indicating that one of the main resistances of the cell is R_k and R_w is too small to affect the direct current resistance, R_{dc}, of the cell. Thus, no drastic effect was observed when R_w decreased with an increase in D_{eff}. However, the condition of $R_k \gg R_w$ does not hold anymore when R_w increases with a decrease in D_{eff}, so that R_w becomes the main resistance and R_k/R_w becomes less than 1, resulting in deviation of the shape of the arc from a true circle especially in the high frequency range, as shown by curve a in Figure 11. The direct current resistance, R_{dc}, also becomes large.

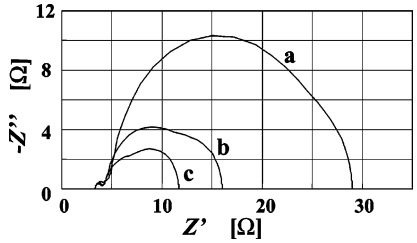

Figure 12. Simulation with variation in Con. Original Con = 0.053. Ratio of Con to the original Con: (a) 3; (b) 1; (c) 1/3.

Simulations with variation in the values of Con were also performed, and the results are shown in Figure 12. The variation in Con affects the shape of the Nyquist plot significantly. Since Con is a common coefficient for both R_k and R_w, the dimensions of the central arc change greatly without changing the ratio of R_k/R_w. A high electron density in the conduction band means a low recombination rate, resulting in a high efficiency in general.

6. Conclusion

(1) Reliable values of the parameters relating to electron transport in dye-sensitized solar cells can be determined from the spectra measured by electrochemical impedance spectroscopy when careful analysis of the measured spectra is done based on the guidelines from the classification and clarification of the characteristics of the impedance equations of the TiO_2 electrode.

Reliable parameter values provide the fundamental information for improving the cell efficiency.

(2) A high electron diffusion coefficient, D_{eff}, a low recombination rate constant, k_{eff}, a much higher recombination resistance, R_k, than the electron diffusion resistance, R_w, and a high electron density, n_s, are the requisites for highly efficient dye-sensitized solar cells.

Acknowledgment. This work was supported by the Strategic University/Industry Alliance of the International Innovation Center, Kyoto University. The conductive ITO glass was kindly provided by Geomatec Co. Ltd.

7. Notation

γ: defined by eq 13 (cm^{-1})
δ: thickness of liquid film (cm)
η: light-to-electricity conversion yield (%)
τ: lifetime of electrons given by eq 4 (s)
τ_{eff}: effective lifetime of electrons defined as $1/k_{eff}$ (s)
φ: phase shift (deg)
ω: modulation frequency (s^{-1})
ω_{max}: peak frequency of arc (s^{-1})
ω_d: defined by eq 4 or eq 18 (s^{-1})
ω_k: defined by eq 4 or eq 18 (s^{-1})
A: electrode area (cm^2)
A_v: Avogadro's constant (mol^{-1})
C^*: concentration of tri-iodide in the bulk electrolyte (mol cm^{-3})
Con: defined by eq 5 or eq 21 (Ω cm s^{-1})
C_p: capacitance at the Pt surface (F)
D: electron diffusion coefficient in TiO_2 (Bisquert model) (cm^2 s^{-1})
D_{eff}: effective electron diffusion coefficient, defined by eq 11 (cm^2 s^{-1})
D_{cb}: electron diffusion coefficient in the conduction band (cm^2 s^{-1})
D_l: diffusion coefficient of tri-iodide in electrolyte (cm^2 s^{-1})

G: generation rate of electron by injection from dye (cm^{-3} s^{-1})
$[I_2]$: concentration of iodine (mol cm^{-3})
ΔI: modulated current (A)
ΔJ: flux of modulated electrons (A cm^{-2})
J: flux of electrons (A cm^{-2})
$\tilde{J}$: modulated flux of electrons (A cm^{-2})
J_{sc}: short circuit current density (mA cm^{-2})
k_1: rate constant for trapping (s^{-1})
k_2: rate constant for detrapping (s^{-1})
k_r: rate constant for recombination from the trap state (model by Kern et al.) (cm^3 s^{-1})
k_{eff}: effective rate constant for recombination given by eq 12 (s^{-1})
k_B: Boltzmann's constant (J K^{-1})
L: thickness of TiO_2 film (cm)
n: conduction band electron density (cm^{-3})
$\tilde{n}$: modulated conduction band electron density (cm^{-3})
n_s: steady-state electron density in the conduction band (cm^{-3})
Δn: amplitude of modulated electron density in the conduction band (cm^{-3})
N: electron density in the trap state (cm^{-3})
N_s: steady-state electron density in the trap state (cm^{-3})
ΔN: modulated electron density in the trap state (cm^{-3})
q: elementary charge (C)
r_p: resistance at the Pt surface (Ω)
R_D: dc resistance of impedance of diffusion of tri-iodide, defined by eqs 33 and 34 (Ω)
R_w: electron transport resistance in TiO_2 (Ω)
R_k: charge-transfer resistance related to recombination of electron (Ω)
R_{dc}: direct current resistance (Ω)
S: defined by eq 17 (V cm^3 $s^{1/2}$)
T: absolute temperature (K)
V_{oc}: open circuit voltage (V)
Z: impedance of the TiO_2 electrode (Ω)
Z_p: impedance of the Pt electrode (Ω)
Z_N: finite Warburg impedance (Ω)
Z': real part of impedance (Ω)
Z'': imaginary part of impedance (Ω)

References and Notes

(1) Kern, R.; Sastrawan, R.; Ferber, J.; Stangl, R.; Luther, J. *Electrochim. Acta* **2002**, *47*, 4213−4225.
(2) Bisquert, J. *J. Phys. Chem. B* **2002**, *106* (2), 325−333.
(3) Bisquert, J.; Garcia-Belmonte, G.; Fabregat-Santiago, F.; Bueno, P. R. *J. Electroanal. Chem.* **1999**, *475*, 152−163.
(4) Fabregat-Santiago, F.; Bisquert, J.; Garcia-Belmonte, G.; Boschloo, G.; Hagfeldt, A. *Sol. Energy Mater. Sol. Cells* **2005**, *87*, 117−131.
(5) van de Lagemaat, J.; Park, N.-G.; Frank, A. J. *J. Phys. Chem. B* **2000**, *104* (9), 2044−2052.
(6) Hoshikawa, T.; Yamada, M.; Kikuchi, R.; Eguchi, K. *J. Electroanal. Chem.* **2005**, *577*, 339−348.
(7) Hoshikawa, T.; Yamada, M.; Kikuchi, R.; Eguchi, K. *J. Electrochem. Soc.* **2005**, *152*, E68−E73.
(8) Hauch, A.; Georg, A. *Electrochim. Acta* **2001**, *46*, 3457−3466.
(9) Fang, X.; Ma, T.; Guan, G,; Akiyama, M.; Kida, T.; Abe, E. *J. Electroanal. Chem.* **2004**, *570*, 257−263.
(10) Han, L.; Koide, N.; Chiba, Y.; Mitate, T. *Appl. Phys. Lett.* **2004**, *84*, 2433−2435.
(11) Frank, A. J.; Kopidakis, N.; van de Lagemaat, J. *Coord. Chem. Rev.* **2004**, *248*, 1165−1179.
(12) Wang, P.; Zakeeruddin, S. M.; Comte, P.; Charvet, R.; Humphry-Baker, R.; Gratzel, M. *J. Phys. Chem. B* **2003**, *107*, 14336−14341.
(13) Fisher, A. C.; Peter, L. M.; Ponomarev, E. A.; Walker, A. B.; Wijayantha, K. G. U. *J. Phys. Chem. B* **2000**, *104* (5), 949−958.
(14) Huang, S. Y.; Schlichthorl, G.; Nozik, A. J.; Gratzel, M.; Frank, A. J. *J. Phys. Chem. B* **1997**, *101* (14), 2576−2582.
(15) Schlichthorl, G.; Huang, S. Y.; Sprague, J.; Frank, A. J. *J. Phys. Chem. B* **1997**, *101* (41), 8141−8155.
(16) Dloczik, L.; Ileperuma, O.; Lauermann, I.; Peter, L. M.; Ponomarev, E. A.; Redmond, G.; Shaw, N. J.; Uhlendorf, I. *J. Phys. Chem. B* **1997**, *101* (49), 10281−10289.
(17) Peter, L. M.; Ponomarev, E. A.; Franco, G.; Shaw, N. J. *Electrochim. Acta*. **1999**, *45*, 549−560.
(18) Duffy, N. W.; Peter, L. M.; Wijayantha, K. G. U. *Electrochem. Commun.* **2000**, *2*, 262−266.
(19) Jiu, J.; Wang, F.; Sakamoto, M.; Takao, J.; Adachi, M. *J. Electrochem. Soc.* **2004**, *151*, A1653−A1658.
(20) Adachi, M.; Murata, Y.; Takao, J.; Jiu, J.; Sakamoto, M.; Wang, F. *J. Am. Chem. Soc.* **2004**, *126* (45), 14943−14949.
(21) Wang, Q.; Moser, J.-E.; Gratzel, M. *J. Phys. Chem. B* **2005**, *109* (31), 14945−14953.
(22) Nelson, I. V.; Iwamoto, T. *J. Electroanal. Chem.* **1964**, *7*, 218−221.
(23) Datta, J.; Bhattacharya, A.; Kundn, K. K. *Bull. Chem. Soc. Jpn.* **1988**, *61*, 1735−1742.